JOURNAL OF SOLID STATE CHEMISTRY 119, 1–7 (1995)

Structure of Calcium Aluminate Sulfate $Ca_4Al_6O_{16}S$

Nicholas J. Calos,*,† Colin H. L. Kennard,†,[1] Andrew K. Whittaker,‡ and R. Lindsay Davis§

*Centre for Microscopy and Microanalysis, †Department of Chemistry, and ‡Centre for Magnetic Resonance, The University of Queensland, Brisbane, Q 4072, Australia; and §ANSTO, Private Mail Bag 1, Menai, New South Wales, Australia

Received May 20, 1994; in revised form February 8, 1995; accepted February 9, 1995

IN MEMORIAM, HENRY ROSSELL

The commensurately modulated structure of polycrystalline calcium aluminate sulfate was determined using spectroscopic and electron microscopic information and calculations with the bond-valence method. The neutron powder diffraction data were refined by the Rietveld profile technique. Calcium aluminate sulfate, $Ca_4Al_6O_{16}S$, MW = 2440 Da, orthorhombic, *Pcc*2, a = 13.028(3) Å, b = 13.037(3) Å, c = 9.161(2) Å, U = 1556(1) Å^3, Z = 4, Dc = 2.60 g cm^3, λ (neutron) = 1.893 Å (Ge monochromated), $\mu R_{neutron}$ = 0.42, R_{Bragg} = 0.046, R_p = 0.06, R_{wp} = 0.08, is a twofold superstructure of sodalite which is generated by z modulation of the framework along [1 1 0] of the cubic subcell. © 1995 Academic Press, Inc.

INTRODUCTION

The molecular sieve properties of the class of compounds known as zeolites have a wide range of uses from water treatment to animal feed and soil nutrient. The usefulness of a particular zeolite is attributed to its pore size, which is a function of the packing of aluminosilicate cages within the unit cell. The composition of the cage unit defines the zeolite species. In the course of a recent study of members of the zeolite family, a synthetic sodalite member, polycrystalline calcium aluminate sulfate (CAS), using the terminology of Depmeier (6), was prepared. This work reports on the structural determination of this compound.

EXPERIMENTAL

The infrared spectrum of the powdered material dispersed in a CsI disk was measured with a Perkin–Elmer Fourier transform infrared spectrometer (FTIR 1600) from 4000–400 cm^{-1}. Magic angle solid state nuclear magnetic resonance spectroscopy (MASS-NMR) was carried out with a Bruker MLS 300 spectrometer. Selected area and convergent beam electron diffraction (SAED, CBED) patterns were obtained using a Philips TEM 400 operating at 120 kV. Lattice imaging was carried out with a JEOL JEM 4000FX analytical electron microscope (AEM). Neutron diffraction data of a powder sample of CAS, packed in a 5-mm-diameter vanadium canister, were collected at ANSTO's HIFAR facility using the high resolution powder diffractomer (HPRD). The diffraction pattern was measured from −1.9° to 160.1° in 2θ in 0.05° steps, λ = 1.893 Å, Ge monochromator. Programs used for structure refinement were STRUMO (2) and a locally modified version of LHPM1 (10). Multislice image calculations were performed using the EMS suite of programs (15).

RESULTS AND DISCUSSION

Infrared Spectroscopy

Multiple SO_4 stretching bands were observed in the infrared spectrum (Table 1, 1154 cm^{-1} 1140 cm^{-1}, and 1118 cm^{-1}), which corresponded to the ν_3 mode (ν_d) of the tetrahedral (T_d) SO_4 group. The multiplicity implied F_2 symmetry for the SO_4 group by comparison to the infrared spectra of anhydrite ($CaSO_4$), celestite ($SrSO_4$), and barite ($BaSO_4$) (1). A bond length for S–O ≈ 1.475 Å was indicated. The multiple bands of the $\nu_3(AlO_4)$ modes (9) at ca. 850 cm^{-1} suggested the loss of $\bar{4}$ symmetry about Al. The degeneracy of all tetrahedral models is lost, indicating the unsuitability of a cubic model for CAS (however disordered).

Magic Angle Solid State Nuclear Magnetic Resonance Spectroscopy

The solid^{27} Al MASS-NMR spectrum of CAS is complex (Fig. 1) and different from the cubic and tetragonal phase spectra reported for the sodalites, $Sr_4(Al_6O_{12})CrO_4$ (SACr) and $Sr_4(Al_6O_{12})WO_4$ (SAW) by van der Klink *et al.* (16). The spectrum consists of a single sharp peak with two shoulders to the high-field side, surrounded by the weaker spin sidebands. At least two types of AlO_4 groups are present according to the appearance of the spectrum. A Jager (11) analysis of the satellite transitions

[1] To whom correspondence should be addressed.

0022-4596/95 $12.00

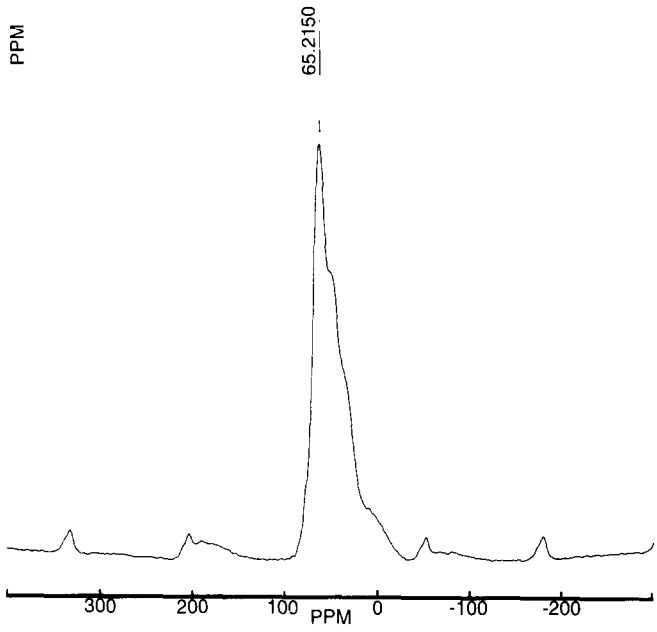

FIG. 1. ^{27}Al MASS–NMR spectrum of CAS.

suggested that chemical shifts of the "symmetric" and "nonsymmetric" Al nuclei are ca. 73 and 62 ppm, respectively. The sharp signal at 65.2 ppm implied an orthorhombic symmetry containing Al nuclei at symmetry axes (by analogy to the system studied by van der Klink *et al.* (16)).

TABLE 1
IR Absorption Maxima and Assignments for CAS

ν_{max}(cm^{-1})	Assignment	
1154	$\nu_3(SO_4)$	
1140	$\nu_3(SO_4)$	
1118	$\nu_3(SO_4)$	
880	$\nu_3(AlO_4)$	$\equiv \nu_{as}$(T–O–T)
857	$\nu_3(AlO_4)$	
741	$\nu_1(AlO_4)$	$\equiv \nu_s$(T–O–T)
658	$\nu_1(AlO_4)$	
646	$\nu_1(AlO_4)$	
609	$\nu_1(AlO_4)$	
588	$\nu_1(SO_4)$	
423	$\nu_2(SO_4)$; $\nu_4(AlO_4)$	$\equiv \delta$(O–T–O)

Electron diffraction

CBED patterns of $[0\ 0\ 1]_{cube}$ (Fig. 2) showed an apparent fourfold symmetry with two mirror planes orthogonal to each other. Therefore, diffraction groups $4mm1_R$ or $4mm$ were possible (point groups $4mm$, $4/mm$, or $m3m$; Buxton *et al.* (3)) at this stage. Closer inspection of patterns from independent samples showed very faint defect lines just inside the first-order Laue zone (FOLZ) ring, which reduced the whole pattern symmetry to $2mm$, giving the diffraction group 4_Rmm_R. Putting aside the assumption that the bright field symmetry was not $4mm$, diffraction groups $2mm$ and $2mm1_R$ are also possible. This gives the point group $\bar{4}2m$, $\bar{4}3m$, mmm, and $mm2$.

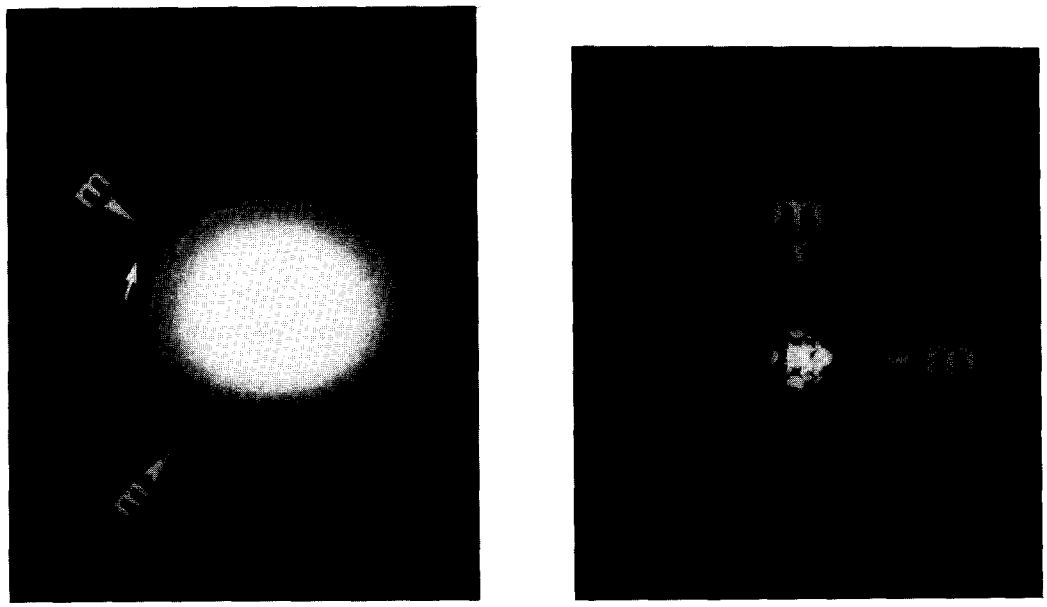

FIG. 2. [0 0 1] CBED whole pattern of CAS with $2mm$ symmetry, and the bright field pattern. (Note faint defect line, arrowed.)

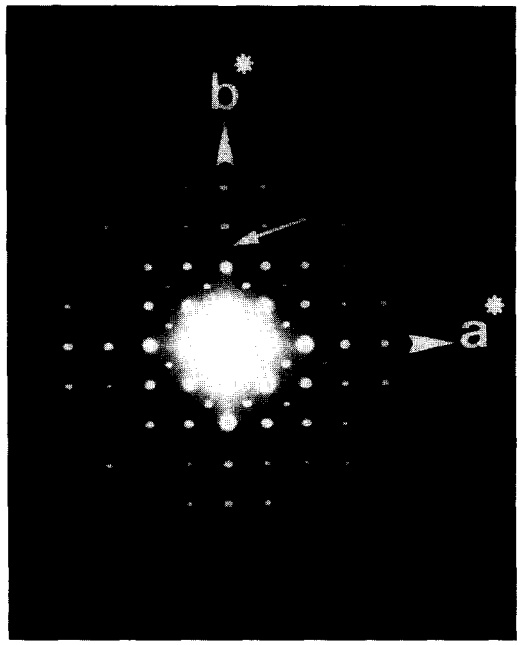

FIG. 3. [0 0 1] SAED pattern of CAS, with faint 13Å superstructure peak (arrowed).

Point groups $4/mmm$ and $m3m$ cannot be considered since the tetrads of these groups do not contain the diffraction groups under consideration (3). SAED patterns showed that CAS clearly had a doubled cubic subcell along $[1\ 1\ 0]_{cube}$ (Fig. 3). Because $(h\ k\ 0) \neq (-k\ h\ 0)$ the symmetry must be orthorhombic or lower. Twinning was frequently observed in the SAED patterns generally about the $\{3\ 1\ 1\}_{orth}$, which corresponded to the $\{2\ 1\ 1\}_{cube}$.

Neutron diffraction

Halstead and Moore (8) proposed a cubic cell for CAS, indexed as $P4_132$ with $a = 18.41$ Å. Kondo (12) suggested a cubic $I23$ structure solution with $a = 9.19$ Å, although this work took no account of the possible superstructure recognized by Halstead and Moore (18) and by Saalfeld and Depmeier (14). A single-crystal XRD study by Wang *et al.* (17) yielded an average cubic structure with the apparent disorder in the Ca position, an artifact of the superstructure. Neutron and X-ray diffraction patterns may be indexed on a 13 × 13 × 9 Å orthogonal cell. Relevant information is listed in Tables 2 and 3.

Electron diffraction patterns (*vide ultra*) indicated a point group of $mm2$ for the cell, with dimensions ≈ 13 × 13 × 9 Å, which represents a superstructure along $[1\ 1\ 0]_{cube}$. Depmeier (7) described the probable breakdown of symmetry in sodalites from cubic $I\bar{4}3m$ through maximal subgroups $Fmm2$, $Abm2$, to $Aba2$ or $Pcc2$. The $Aba2$ symmetry may arise through doubling of one of the superstructure 13 Å axes as formed in CAW (5). Since no such 26 Å dimension was observed in the SAED patterns, only $Fmm2$, $Abm2$, and $Pcc2$ were considered here. Reflections belonging to the primitive lattice could be observed and indexed in the Guinier photograph, so $Pcc2$ was the only choice. Extra faint and diffuse lines belonging to $CaAl_2O_4$, $CaAl_4O_7$, ettringite, gypsum, bassanite, and portlandite (i.e., hydrolysis products), and Pt from the sample holder could also be observed. The superstructure cell based on Guinier photograph line positions (Rossell (13) was $a = 13.028(3)$ Å, $b = 13.037(3)$ Å, $c = 9.161(2)$ Å.

Based on a study of distortions available to sodalites (6), superstructure formation through z-modulation of atomic positions was deemed most likely in CAS. Atomic positions for two cubic subcells (as found by Wang *et al.* (17) were generated and transformed into the appropriate coordinates for the 13 × 13 × 9 Å cell, and the origin was shifted by $\frac{1}{4}, \frac{1}{4}, 0$. This origin shift placed two Al atoms on diads, consistent with the NMR finding. A set of unique coordinates appropriate for $Pcc2$ were selected. In order to generate the superstructure, the Al centers at general positions were shifted in z by 0.01. This displacement gave the framework a "kinked," or modulated, appearance. Oxygen positions of the framework were then refined around these fixed Al centers, according to least-squares minimization of bond-valence differences around each atom. Ca atoms were refined to fit into the modulated framework, then the sulfate groups were done and the process was repeated to iteratively achieve a best-fit structure according to the bond-valences about each atom.

This model gave rise to appropriately placed and adequately sized superstructure peaks for subsequent Rietveld refinement. Rietveld refinement on neutron data yielded a structure which fitted to an R_{Bragg} factor of 0.03. The lighter atoms (Al and S) refined to unreasonable positions and gave unreasonable Al–O and S–O bond lengths. However, using bond-valences, a final round of refinement of Al and S and then Ca positions produced a structure which fitted the neutron diffraction patterns with slightly higher but still acceptable refinement indices ($R_p = 0.06$ and $R_{Bragg} = 0.046$). This structure had physically meaningful Al–O, S–O bond distances and angles (Fig. 4). The structure was also consistent with the NMR and IR observations previously discussed. Furthermore, the material on which the neutron diffraction data were collected was essentially pure, with little or no hydrolysis as seen in later X-ray diffraction experiments. The small amount of H found in IR and NMR was shown by secondary ion mass spectrometry (SIMS) and static SIMS to be surface hydroxylation.

TABLE 2
CAS *Pcc*2 Bond-Valence-Based Neutron Refinement

Atom	Site	Symm	x	y	z	B_{iso}	N	
S	4*e*	1	0.25366	0.24870	0.98218	1.9(4)	1.0	(fixed)
$O_S(1)$	4*e*	1	0.729(3)	0.317(3)	0.612(9)	7.5(3)	1.0	
$O_S(2)$	4*e*	1	0.838(5)	0.184(4)	0.46(1)	7.5(3)	1.0	
$O_S(3)$	4*e*	1	0.770(4)	0.336(3)	0.379(9)	7.5(3)	1.0	
$O_S(4)$	4*e*	1	0.651(4)	0.201(4)	0.417(9)	7.5(3)	1.0	
Ca(1)	4*e*	1	0.058(2)	0.251(3)	0.149(8)	2.1(2)	1.0	
Ca(2)	4*e*	1	0.237(2)	0.926(2)	0.286(9)	2.1(2)	1.0	
Ca(3)	4*e*	1	0.257(3)	0.512(3)	0.254(8)	2.1(2)	1.0	
Ca(4)	4*e*	1	0.483(2)	0.253(3)	0.228(8)	2.1(2)	1.0	
Al(1)	2*d*	2	$\frac{1}{2}$	$\frac{1}{2}$	0.23(1)	0.4(3)	0.5	
Al(2)	2*c*	2	$\frac{1}{2}$	0	0.25(1)	0.4(3)	0.5	
Al(3)	2*a*	2	0	0	0.205(9)	0.4(3)	0.5	
Al(4)	2*b*	2	0	$\frac{1}{2}$	0.20(1)	0.4(3)	0.5	
Al(5)	4*e*	1	0.627(4)	0.121(4)	−0.004(9)	0.2(2)	1.0	
Al(6)	4*e*	1	0.122(4)	0.625(3)	0.949(9)	0.2(2)	1.0	
Al(7)	4*e*	1	0.369(4)	0.629(3)	0.98(1)	0.2(2)	1.0	
Al(8)	4*e*	1	0.122(4)	0.876(3)	0.96(1)	0.2(2)	1.0	
O(1)	4*e*	1	0.400(2)	0.246(2)	0.438(8)	1.38(5)	1.0	
O(2)	4*e*	1	0.567(2)	0.409(3)	0.140(8)	1.38(5)	1.0	
O(3)	4*e*	1	0.555(2)	0.105(2)	0.155(8)	1.38(5)	1.0	
O(4)	4*e*	1	0.755(2)	0.590(2)	0.504(8)	1.38(5)	1.0	
O(5)	4*e*	1	0.596(2)	0.443(2)	0.826(8)	1.38(5)	1.0	
O(6)	4*e*	1	0.907(2)	0.446(2)	0.802(8)	1.38(5)	1.0	
O(7)	4*e*	1	0.757(3)	0.902(2)	0.536(8)	1.38(5)	1.0	
O(8)	4*e*	1	0.901(2)	0.034(2)	0.824(8)	1.38(5)	1.0	
O(9)	4*e*	1	0.608(2)	0.033(2)	0.854(8)	1.38(5)	1.0	
O(10)	4*e*	1	0.103(2)	0.247(2)	0.391(8)	1.38(5)	1.0	
O(11)	4*e*	1	0.953(2)	0.115(2)	0.125(8)	1.38(5)	1.0	
O(12)	4*e*	1	0.948(2)	0.389(2)	0.110(8)	1.38(5)	1.0	

Note. a = 13.0409(8) Å, b = 13.0393(9) Å, c = 9.1692(3) Å, neutron refinement; a = 13.028(3) Å, b = 13.037(3) Å, c = 9.161(2) Å, Guinier cell. Gaussian peak width parameters: Lorentzian component γ = 0.024(3); Asymmetry parameter A = 0.170(4). Gaussian peak widths refer to the Caglioti *et al.* (4) formula: FWHM = $\sqrt{(-0.9(2) \times 10^{-2} \tan^2\theta + 0.69(3) \times 10^{-1})}$; R_{Bragg} = 0.046; R_p = 0.063; R_{wp} = 0.080.

Description of Structure

The cages of SAW and $Sr_4(Al_6O_{12})MoO_4$, SAM, are nearly fully expanded and they possess small tilt angles (6). Some of the constituent AlO_4 tetrahedra deform due to "conformational shearing," giving rise to superstructures. In contrast, CAW (5) follows partial collapse of cage tetrahedra to generate a superstructure. In the superstructure of CAS, concerted tilting of the AlO_4 tetrahedra leads to the modulated structure reported by Depmeier (5). CAS has the largest tilt angle for the cage tetrahedra of the aluminate sodalities so far determined (6). The modulation of the cage structure may be clearly seen in Fig. 5.

Lattice Imaging

Multislice image calculations showed that pseudocubic projections of CAS have essentially no superstructure until very large values of thickness of defocus. There was no appreciable difference between $\langle 1\ 1\ 0 \rangle_{orthorhombic}$, $\langle 0\ 0\ 1 \rangle_{orthorhombic}$, and $\langle 1\ 0\ 0 \rangle_{cubic}$ calculated images (Fig. 6) in thin crystal sections. Calculated images may be compared to the observed $\langle 1\ 0\ 0 \rangle_{cubic}$ image with no apparent superstructure (Fig. 6d). Superstructure becomes evident only in the pseudocubic projections at quite large crystal thickness values. The $\langle 1\ 1\ 0 \rangle_{orthorhombic}$ calculations may be compared to the $\langle 1\ 0\ 0 \rangle_{cubic}$ calculations and the observed image for equivalent thickness and defocus values (Fig. 7). The differences between the orthorhombic and cubic models appear at thickness t = 73.8 nm (Fig. 7c). In contrast to Wang *et al.* (17, 18), the lattice image analyses in conjunction with the neutron diffraction findings show CAS to be an ordered structure in which the Ca atoms occupy discrete sites within a supercell with *Pcc*2 symmetry.

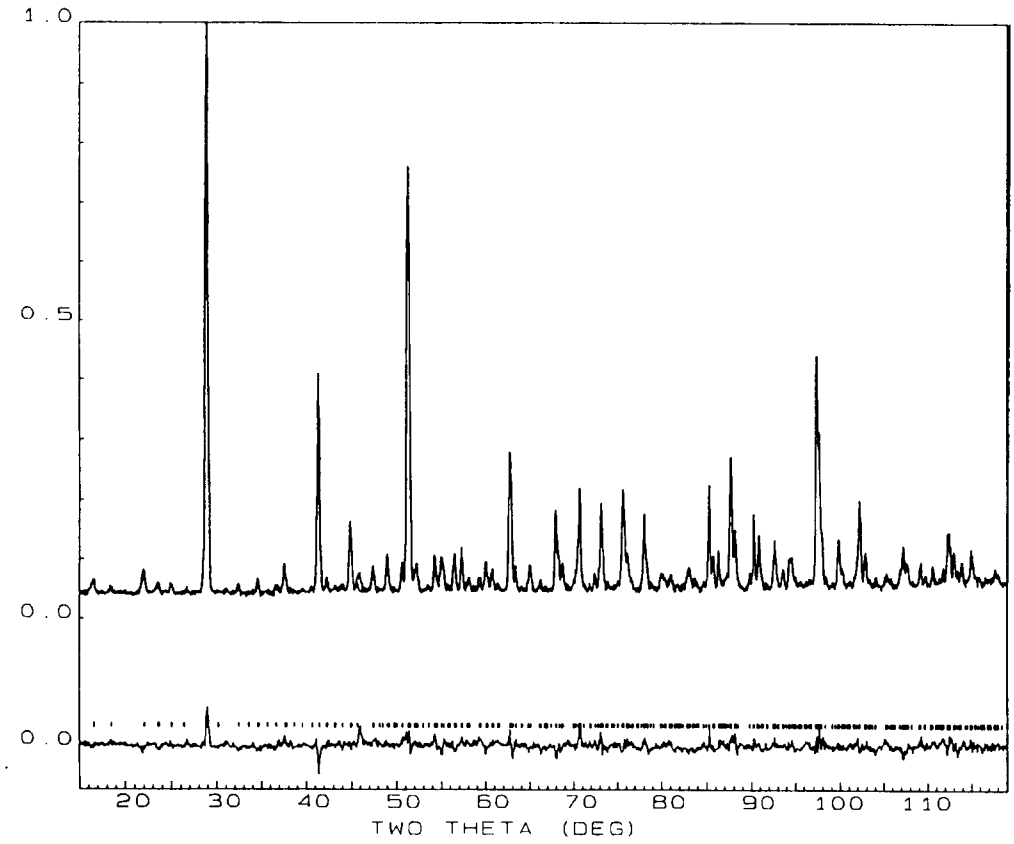

FIG. 4. Rietveld refined neutron diffraction profile of CAS.

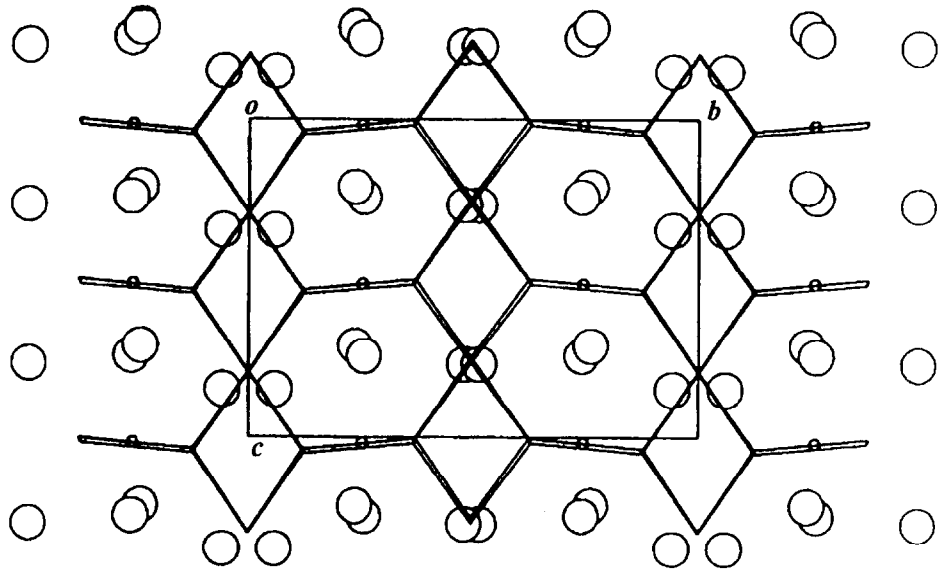

FIG. 5. [1 0 0] projection of the structure of polycrystalline calcium aluminate sulfate, CAS. Ca, large circles; SO_4 centers, small circles; AlO_4 centers, linking lines.

FIG. 6. HRTEM images of CAS using t = 3.7 nm, Δf = −20 nm, C_s = 3.4 mm, d = 10 nm^{-1}, Δ = 10 nm sec = 1.0 mrad; (a) calculated $\langle 1\ 1\ 0\rangle_{\text{orthorhombic}}$, (b) calculated $\langle 0\ 0\ 1\rangle_{\text{orthorhombic}}$, (c) calculated $\langle 1\ 0\ 0\rangle_{\text{cubic}}$, (d) observed $\langle 1\ 0\ 0\rangle_{\text{cubic}}$.

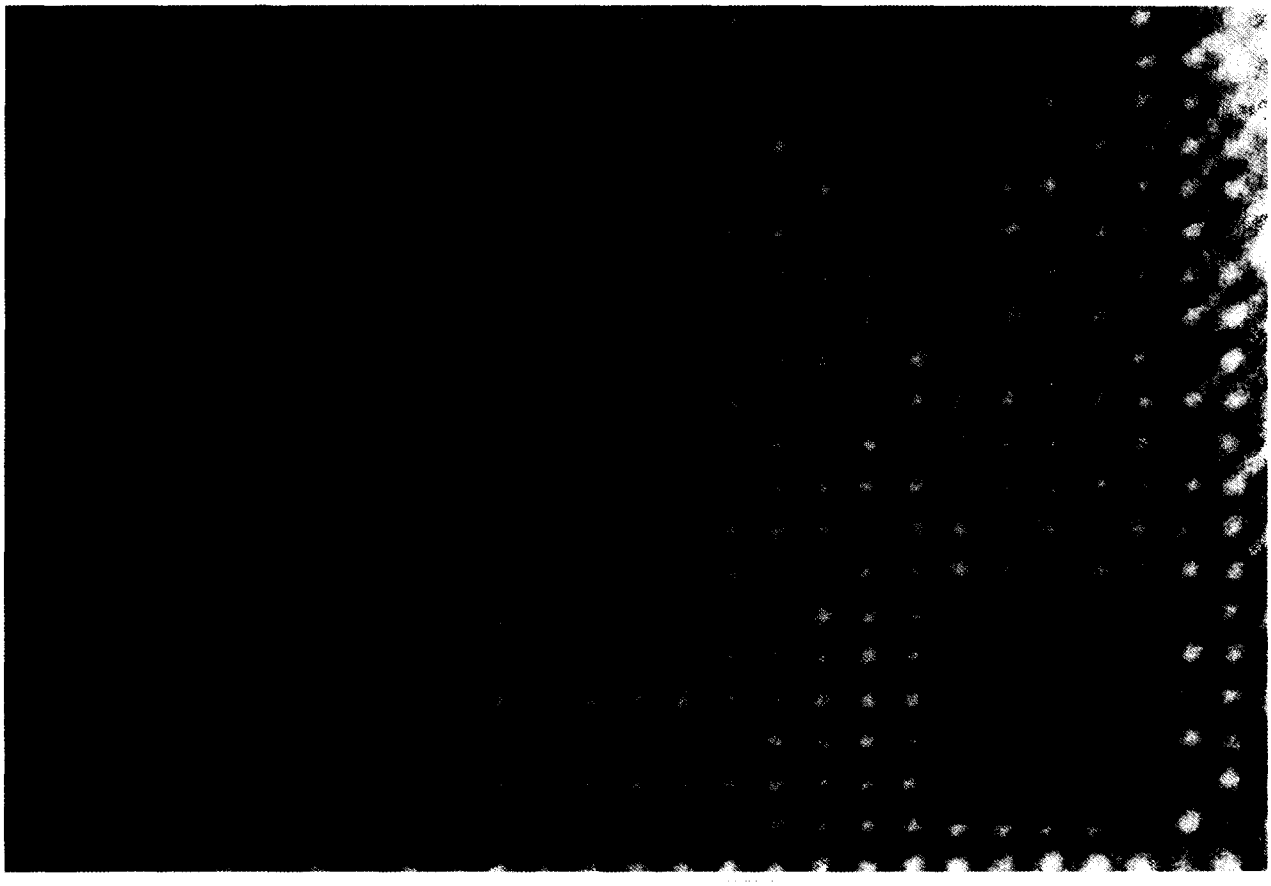

FIG. 7. HRTEM images of CAS using t = 73.8 nm, Δf = −20 nm, C_S = 3.4 mm, d = 10 nm^{-1}, Δ = 10 nm sec = 1.0 mrad; (a) calculated $\langle 1\ 1\ 0\rangle_{\text{orthorhombic}}$, (b) calculated $\langle 1\ 0\ 0\rangle_{\text{cubic}}$, (c) observed $\langle 1\ 1\ 0\rangle_{\text{orthorhombic}}$.

TABLE 3
Selected Bond Distances (Å) and Bond Angles (°) for CAS

S–O_S(1)	1.51(7)	O_S(1)–S–O_S(2)	123(10)	O_S(2)–S–O_S(3)	101(9)
S–O_S(2)	1.48(4)	O_S(1)–S–O_S(3)	94(6)	O_S(2)–S–O_S(4)	113(11)
S–O_S(3)	1.51(6)	O_S(1)–S–O_S(4)	116(9)	O_S(3)–S–O_S(4)	103(9)
S–O_S(4)	1.51(7)				
Al(1)–O(2)	1.69(18)				
Al(1)–O(5)	1.69(10)		Al(6)–O(4)	1.74(12)	
			Al(6)–O(6)	1.68(11)	
Al(2)–O(3)	1.76(20)		Al(6)–O(10)	1.77(17)	
Al(2)–O(9)	1.77(20)		Al(6)–O(12)	1.74(22)	
Al(3)–O(8)	1.75(20)		Al(7)–O(1)	1.73(10)	
Al(3)–O(11)	1.78(23)		Al(7)–O(2)	1.76(17)	
			Al(7)–O(4)	1.71(8)	
Al(4)–O(6)	1.70(11)		Al(7)–O(5)	1.76(8)	
Al(4)–O(12)	1.78(23)				
			Al(8)–O(7)	1.75(12)	
Al(5)–O(1)	1.75(14)		Al(8)–O(8)	1.76(21)	
Al(5)–O(3)	1.75(21)		Al(8)–O(10)	1.75(17)	
Al(5)–O(7)	1.76(12)		Al(8)–O(11)	1.78(23)	
Al(5)–O(9)	1.75(21)				
Ca(1)–O(6)	2.94(34)		Ca(2)–O(7)	2.32(15)	
Ca(1)–O(10)	2.29(34)		Ca(2)–O(8)	2.31(26)	
Ca(1)–O(11)	2.26(41)		Ca(2)–O(9)	2.54(29)	
Ca(1)–O(12)	2.33(42)		Ca(2)–O(11)	2.93(37)	
Ca(1)–O_S(1)	2.93(37)		Ca(2)–O_S(2)	2.39(22)	
Ca(1)–O_S(2)	2.34(35)		Ca(2)–O_S(4)	2.52(23)	
Ca(3)–O(2)	2.72(29)		Ca(4)–O(1)	2.21(18)	
Ca(3)–O(4)	2.51(15)		Ca(4)–O(1)	3.06(25)	
Ca(3)–O(4)	2.66(16)		Ca(4)–O(2)	2.44(29)	
Ca(3)–O(5)	2.22(13)		Ca(4)–O(3)	2.24(28)	
Ca(3)–O(6)	2.35(13)		Ca(4)–O(5)	2.83(20)	
Ca(3)–O_S(3)	2.32(18)		Ca(4)–O_S(4)	2.87(28)	

ACKNOWLEDGMENTS

The authors thank Dr. F. Hanic of the Slovak Academy of Sciences, Bratislavia, for the sample of calcium aluminate sulfate and the Australian Institute for Nuclear Science and Technology for financial support. Henry Rossell is acknowledged for the Guinier photography.

REFERENCES

1. H. H. Adler and P. F. Kerr *Am. Mineral*, **50,** 132 (1965).
2. D. Altermatt and I. D. Brown *Acta Crystallogr. Sect. B Struct. Sci.* **41,** 240 (1985).
3. B. F. Buxton, J. A. Eades, J. W. Steeds, G. M. Rackham *Philos. Trans. R. Soc.* **281,** 171 (1976).
4. G. Caglioti, A. Paoletti. and F. P. Ricci *Nucl. Instrum.* **3,** 223 (1958).
5. W. Depmeier, *Acta Crystallogr. Sect. C. Cryst. Struct. Commun.* **40,** 226 (1984).
6. W. Depmeier, *Phys. Chem. Miner.* **15,** 419.
7. W. Depmeier *Z. Kristallogr.* **199,** 75 (1992).
8. P. E. Halstead and A. E. Moore *J. Appl Chem.* **12,** 413 (1962).
9. C. M. B. Henderson and D. Taylor *Spectrochim. Acta, Part A* **35,** 929 (1979).
10. R. J. Hill and C. J. Howard *J. Appl. Crystallogr.* **18,** 173 (1985).
11. C. Jager *J. Magn. Res.* **99,** 353.
12. R. Kondo *J. Ceram. Assoc. Jpn.* **73,** 101 (1965).
13. H. Rossell personal communication, 1991.
14. H. Saalfeld and W. Depmeier (1972), *Krist. Tech.* **7,** 229.
15. P. Stadelmann (1987), *Ultramicroscopy* **21,** 131.
16. J. J. van der Klink, W. S. Veeman, and H. Schmid, *J. Phys. Chem.* **95,** 1508 (1991).
17. Y. G. Wang, H. Q. Ye, K. H. Kuo, X. J. Feng, G. L. Lao, and S. Z. Long, *J. Mater. Sci.* **25,** 5147 (1990).
18. Y. G. Wang, H. Q. Ye, K. H. Kuo, X. J. Feng, G. L. Lao, and S. Z. Long, *J. Mater. Sci.* **26,** 814 (1991).